View metadata, citation and similar papers at core.ac.uk

brought to you by CORE

provided by Tomsk State University Repository

Chinese Journal of Physics 55 (2017) 59–63

Contents lists available at ScienceDirect

Chinese Journal of Physics

journal homepage: www.elsevier.com/locate/cjph

Conduction mechanism of metal-TiO_2–Si structures

V.M. Kalygina [a], I.S. Egorova [a], I.A. Prudaev [a], O.P. Tolbanov [a], V.V. Atuchin [a,b,c,d,*]

[a] Functional Electronics Laboratory, Tomsk State University, Tomsk 634050, Russia
[b] Laboratory of Optical Materials and Structures, Institute of Semiconductor Physics, SB RAS, Novosibirsk 630090, Russia
[c] Laboratory of Semiconductor and Dielectric Materials, Novosibirsk State University, Novosibirsk 630090, Russia
[d] Institute of Chemistry, Tyumen State University, Tyumen 625003, Russia

ARTICLE INFO

Article history:
Received 16 March 2016
Revised 2 August 2016
Accepted 8 August 2016
Available online 26 October 2016

Keywords:
Titanium oxide film
Annealing
Space charge limited current
Charge carrier generation

ABSTRACT

The conduction model has been proposed for the metal-TiO_2–Si (MIS) structures. Rutile films have been prepared on Si substrates by magnetron sputtering of TiO_2 target and annealing in the air at temperatures $T = 800$ and 1050 K. The current-voltage (CVC) and capacitance-voltage characteristics of the structures have been measured over the range of $T = 283$–363 K. At positive potentials on the gate, the conductivity of the MIS structures is determined by the space charge-limited current in the dielectric layer.

© 2016 Published by Elsevier B.V. on behalf of The Physical Society of the Republic of China (Taiwan).

1. Introduction

Functional oxide thin films are of great importance in modern micro- and nanoelectronics, including metal-insulator-semiconductor (MIS) structures [1–13]. Titanium oxide films can be used as the key elements in different electronic devices such as memristors, photovoltaic cells, transparent electrodes and gas sensors. A breakthrough in the development of silicon microelectronic is associated with an increased informative capacity that can be achieved by replacing traditional SiO_2 on dielectrics with high dielectric permitivity ε. One of the possible candidates for the role of an alternative dielectric is a titanium oxide with a band gap of $E_g = (3.0–3.2)$ eV and $\varepsilon = 30–80$ depending on the structure and phase composition. In the present study, the conduction mechanism is evaluated in metal-TiO_2–Si structures.

2. Experimental methods

Titanium oxide film, with thickness $d = 70$ nm, were prepared by magnetron sputtering on a silicon epitaxial layer with donor concentration $N_d = 7 \times 10^{14}$ cm^{-3}. The TiO_2 ceramic disc was used as a target for sputtering. The sample preparation details can be found elsewhere [14–16]. After titanium oxide deposition, the Si substrate with the dielectric film was divided into several parts. One part was not subjected to annealing and two parts were annealed in the Ar atmosphere for 30 min at $T_a = 800$ or 1050 K.

The structure and phase composition of TiO_2 films were determined by X-ray diffraction analysis using a Shimadzu XRD-Position 6000 with Cu Kα ($\lambda = 1.5405$ Å) radiation. For the measurement of electrical characteristics, the V/Ni electrodes were deposited by electron beam evaporation on both TiO_2 and Si surfaces. The diameter of the electrode to the TiO_2 gate

* Corresponding author at: Institute of Semiconductor Physics, Novosibirsk 630090, Russia. Fax: +7 (383) 3332771.
E-mail addresses: atuchin@isp.nsc.ru, atuchin@thermo.isp.nsc.ru (V.V. Atuchin).

http://dx.doi.org/10.1016/j.cjph.2016.08.011
0577-9073/© 2016 Published by Elsevier B.V. on behalf of The Physical Society of the Republic of China (Taiwan).

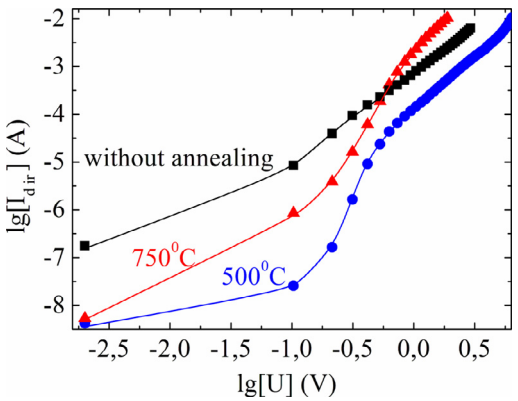

Fig. 1. CVC of unannealed and annealed samples.

Table 1
The slope of the CVC in the second portion, dielectric permitivity, the energy position of the recombination level and trap concentration in TiO_2 films.

Annealing mode	m value for II section of CVC	Relative dielectric permitivity ε	ΔE_{ts}, eV	N_t, cm^{-3}
Without annealing	2.8	32	0.44 ± 0.07	$7.0 \cdot 10^{16}$
800 K	4.9	46	0.52 ± 0.04	$3.3 \cdot 10^{17}$
1050 K	4.6	44	0.81 ± 0.01	$2.6 \cdot 10^{17}$

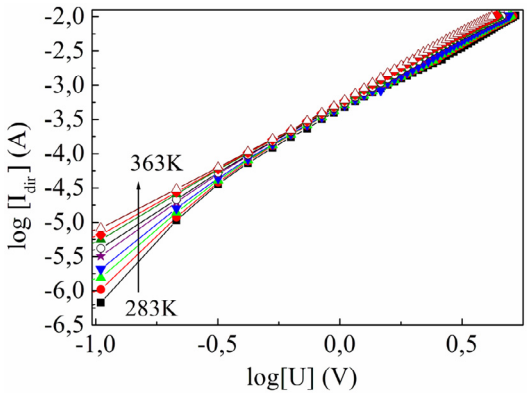

Fig. 2. The temperature dependence of the direct current of the unannealed sample.

was 1.15 mm, and the area was $S = 1.04 \times 10^{-2}$ cm^2. The experiment included the measurements of the current-voltage (CVC) and capacitance-voltage characteristics in the temperature range of $T = 283$–363 K using a Keithley 2636A Source-meter and a thermostat with the accuracy of $T = 0.1$ K.

3. Results and discussion

As deposited titanium oxide films are amorphous. According to XRD spectra, the sample annealed at 800 K possesses a combination of the amorphous phase background and low intensity diffraction peaks. The peaks match well those of the PDF card (No.:43–1012) and can be revealed at $2\theta = 25.2°$, 27.4° and 56.7° which belong to crystallites of anatase and rutile, as shown in Fig. S1. After annealing at 1050 K, the amorphous phase disappears, and the film becomes polycrystalline rutile (Fig. S2). Thus, the annealing temperature mobility of the oxygen atoms increases and, at the same oxygen concentration, the amorphous-crystalline film transforms into a polycrystalline phase.

There are three sections at the direct current-voltage characteristics $I \sim U^m$ (Fig. 1), regardless of the annealing temperature. The first section is observed at $U > 0.1$ V with $m \approx 1$. In the second section ($0.1 \leq U \leq 1.0$ V), value m depends on the annealing temperature and lies in the range of 2.8–4.9 (Table 1), and it reduced to 2 at 0.9 V (third section).

Direct current (I_{dir}) weakly depends on temperature in the voltage range corresponding to the second CVC section. The temperature dependence of I_{dir} for the unannealed sample is shown in Fig. 2. Similar results were obtained for the structures after annealing at $T_a = 800$ and 1050 K. At negative potentials at the gate, the dependence of reverse current I_{rev} on voltage

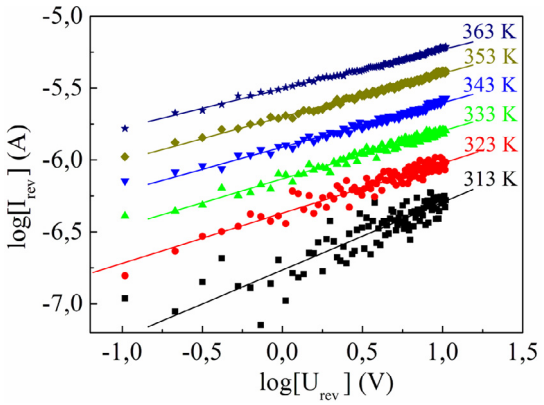

Fig. 3. The temperature dependence of the reverse current of the unannealed sample.

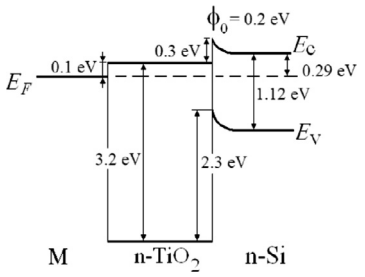

Fig. 4. Energy diagram of the TiO_2-n-Si structure.

is represented by a line with the slope of $m = 0.5$ over the range of $U = 1\times10^{-3}$–10 V. With a temperature increase, the reverse current increases exponentially (Fig. 3).

The TiO_2-n-Si energy diagram is shown in Fig. 4. Note the small value of conduction band discontinuity $\Delta E_c = 0.3$ eV and large valence band discontinuity $\Delta E_v = 2.3$ eV, as well as that of a small band bending on the Si surface, which does not exceed 0.2 eV At positive potentials on the gate, electrons are injected from Si into TiO_2. Even at a small bias voltage, the barrier at the TiO_2-n-Si interface becomes insufficient and all voltage is applied to the dielectric film. Thus, the current flow is determined by the processes in TiO_2. From the analysis of current-voltage characteristics, it follows that the TiO_2 film conductivity is determined by the space charge limited current (SCLC) in a dielectric with traps exponentially distributed by energy. The dependence of the current density on voltage is described by expression [17]

$$J = N_c \mu e^{1-l}\left[\frac{\varepsilon\varepsilon_0 l}{N_t(l+1)}\right]^l \left(\frac{2l+1}{l+1}\right)^{l+1}\frac{U^{l+1}}{L^{2l+1}}, \tag{1}$$

where N_c – effective density of states in the conduction band of TiO_2; ε – dielectric permittivity; ε_0 – electric constant; μ – electron mobility; N_t – trap concentration in the TiO_2 film; e – electron charge. According to Eq. (1), $l = m-1$. The weak temperature dependence of the current (Fig. 2) is consistent with the assumption of SCLC. The voltage of transition from the Ohm law to SCLC is described by relation [17]

$$U_{\Omega\to T} = \frac{eL^2}{\varepsilon\varepsilon_0}\left(\frac{l+1}{2l+1}\right)^{(1+l)/l} \times N_t\left(\frac{n_0'}{N_c}\right)^{1/l}\left(\frac{l+1}{l}\right). \tag{2}$$

Using the experimental data and (2), it was found that $N_t = 7.0\times10^{16}$, 3.3×10^{17} and 2.6×10^{17} cm^{-3} for the structures without annealing and annealed at 800 and 1050 K, respectively (Table). For the calculation of N_t, concentration n_0' was assumed to be 10^{17} cm^{-3} and $N_c = 2\times10^{18}$ cm^{-3} [18]. The *C–U* characteristics measured at the frequency of 1 MHz are shown in Fig. 5. The horizontal line marks the capacitance values C_{fb} corresponding to the flat-band voltage (U_{fb}). The flat-band voltage was found using the experimental curves *C* of *U* (Fig. 5) and calculated values C_{fb} in the flat-band mode [19]:

$$C_{fb} = \frac{\varepsilon_s\varepsilon_0 S}{d + \frac{\varepsilon}{\varepsilon_s}L_n}, \tag{3}$$

$$L_n = \sqrt{\frac{kT\varepsilon_s\varepsilon_0}{e^2 n_0}}, \tag{4}$$

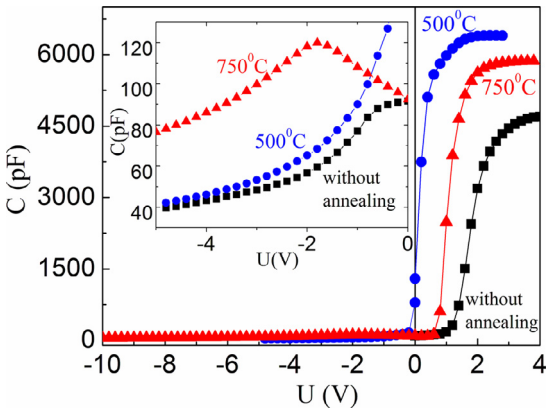

Fig. 5. *C-U* characteristics of the metal TiO_2-n-Si structures. The *C-U* dependence at negative potentials is shown in details in the inset.

where ε_s – the dielectric permittivity of silicon; n_0 - equilibrium electron concentration in Si; k - Boltzmann constant. At $U = 1$ V, the TiO_2-n-Si structures are at the flat band mode. With a further increase of the voltage, the band bending at the Si surface becomes positive and the structure transverses to the enrichment mode.

At negative potentials at the gate, the SCR is formed in the Si region, and the voltage drop is distributed between the TiO_2 film and SCR. The current through structure I_{rev} is due to the electron-hole pair generation in the SCR and is described by expression [20]:

$$I_{rev} \approx I_g = \frac{S e n_i d_{scr}(U)}{\tau_e}, \tag{5}$$

where n_i is charge carriers concentration in the intrinsic semiconductor; d_{scr} (U) is the width of the space charge region; τ_e is effective lifetime.

In the n-semiconductor taking into account that recombinational level is located in the upper half of the forbidden band $\tau_e \approx \frac{1}{\gamma_p N_t} \times \frac{n_1}{n_0}$, where γ_p is hole recomination coefficient; n_0 is electrons equilibrium concentration in Si; $n_1 = N_c \cdot \exp[(E_{ts} - E_c)/kT]$ is equilibrium concentration of electrons in case the Fermi level F matches the trap level E_{ts}. In the range of temperatures corresponding to exhaustion of N_d temperature dependence τ_e is defined by n_1.

The voltage drop at the space charge region (U_{scr}) is determined by

$$U_{scr} = U - I_g R_d \tag{6}$$

where R_d – the TiO_2 film resistance. The dependence of I_g on the voltage is given by

$$I_g = A \cdot \sqrt{\varphi_s + (U - I_g R_d)}, \tag{7}$$

where φ_s is surface potential at the TiO_2–Si interface,

$$A = \frac{S e n_i}{\tau_e} \sqrt{\frac{2\varepsilon_s \varepsilon_0}{e N_d}}. \tag{8}$$

Solving Eq. (7) we can find I_g:

$$I_g = \frac{A^2 R_d}{2} \left[\sqrt{1 + \frac{4(\varphi_s + U)}{A^2 R_d^2}} - 1 \right]. \tag{9}$$

Numerical analysis shows that, in (9), $AR_d << 1$ and

$$I_{rev} = I_g \approx A\sqrt{\varphi_s + U}. \tag{10}$$

At $U >> \varphi_s = 0.2$ V, the CVC has a linear form on the double logarithmic scale with the slope equal to 0.5, which corresponds to the data in Fig. 3.

The temperature dependence of the reverse current is determined by

$$A = C \cdot \exp(-E_g/2kT) \times \exp[(E_c - E_{ts})/kT], \tag{11}$$

C is the constant which isn't depending on temperature According to Eqs. (10) and (11), the reverse current at $U > \varphi_s$ should increase with temperature exponentially with activation energy $(E_{ts} - E_i)/k$, где E_i – is the middle of the bandgap. Using the experimental temperature dependence, and Eq. (11), $\Delta E_t = E_c - E_{ts}$ (the energy position of recombination level E_{ts} in reference to the bottom of conduction band E_c in Si) can be found (Table 1). To explain the difference in ΔE_t, the recombination process at the TiO_2–Si interface should be accounted for. The properties of the TiO_2-Si interface are determined

by the oxide phase composition. The ΔE_{ts} values for amorphous and amorphous-crystalline TiO_2 films coincide within the possible error.

In the structures M- TiO_2-n-Si with the rutile film, recombination level E_{ts} is in the lower half of the band gap, which implies a substantial change of the TiO_2-Si interface. Capacitance-voltage and conductance-voltage characteristics at negative potentials at the gate confirm the significant changes at the TiO_2–Si interface by transition from the amorphous to polycrystalline state (inset in Fig. 5). After annealing at 1050 K, a maximum appears in the *C-U* curves at negative voltages indicating a new surface states group emergence (E_{ts}) (not typical of the structures without annealing and after annealing at 800 K). A similar peak is present at negative potentials at *G-U* curves. Special behavior of *C–U* and *G–U* characteristics of TiO_2–Si structures after annealing at 1050 K are explained with an increase in the differences between crystal lattice parameters of a polycrystalline oxide film and silicon.

4. Summary

The influence of annealing temperature of TiO_2 films on the currents in metal-TiO_2–Si structures was investigated. Regardless of the annealing temperature, the conductivity of the structures at positive potentials on the gate is determined by the space charge-limited current in the dielectric. At negative potentials, the current-voltage characteristics are explained by the thermal generation of electron-hole pairs in the space charge region of Si. The properties of TiO_2–Si interface strongly depend on the titanium oxide phase which is determined by the annealing temperature.

Acknowledgment

This work was supported by the Ministry of Education and Science of the Russian Federation (Project No 3.1206.2014).

Supplementary materials

Supplementary material associated with this article can be found, in the online version, at doi:10.1016/j.cjph.2016.08.011.

References

[1] J. Robertson, J. Appl. Phys. 104 (2008) 124111.
[2] C.V. Ramana, V.V. Atuchin, V.G. Kesler, V.A. Kochubey, L.D. Pokrovsky, V. Shutthanandan, U. Becker, R.C. Ewing, Appl. Surf. Sci. 253 (2007) 5368.
[3] V.A. Shvets, V.Sh. Aliev, D.V. Gritsenko, S.S. Shaimeev, E.V. Fedosenko, S.V. Rykhlitski, V.V. Atuchin, V.A. Gritsenko, V.M. Tapilin, H. Wong, J. Non Cryst. Solids 354 (2008) 3025.
[4] V.V. Atuchin, B.M. Ayupov, V.A. Kochubey, L.D. Pokrovsky, C.V. Ramana, Yu.M. Rumiantsev, Opt. Mater. 30 (2008) 1145.
[5] C.V. Ramana, S. Utsunomiya, R.C. Ewing, U. Becker, V.V. Atuchin, V.Sh. Aliev, V.N. Kruchinin, Appl. Phys. Lett. 92 (2008) 011917.
[6] V.M. Kalygina, A.N. Zarubin, V.A. Novikov, Y.S. Petrova, M.S. Skakunov, O.P. Tolbanov, A.V. Tyazhev, T.M. Yaskevich, Semiconductors 44 (2010) 1227.
[7] V.V. Atuchin, A.V. Kalinkin, V.A. Kochubey, V.N. Kruchinin, R.S. Vemuri, C.V. Ramana, J. Vac. Sci. Technol. A 29 (2011) 021004.
[8] V.M. Kalygina, A.N. Zarubin, Y.P. Nayden, V.A. Novikov, Y.S. Petrova, O.P. Tolbanov, A.V. Tyazhev, T.M. Yaskevich, Semiconductors 45 (2011) 1097.
[9] V.H. Mudavakkat, V.V. Atuchin, V.N. Kruchinin, A. Kayani, C.V. Ramana, Opt. Mater. 34 (2012) 893.
[10] V.V. Atuchin, V.N. Kruchinin, Y.H. Wong, K.Y. Cheong, Mater. Lett. 105 (2013) 72.
[11] V.M. Kalygina, V.V. Vishnikina, A.N. Zarubin, Y.S. Petrova, M.S. Skakunov, O.P. Tolbanov, A.V. Tyazhev, T.M. Yaskevich, Russ. Phys. J. 56 (2014) 984.
[12] V.Sh. Aliev, S.G. Bortnikov, I.A. Badmaeva, J. Appl. Phys. 115 (2014) 204511.
[13] V.M. Kalygina, V.V. Vishnikina, Y.S. Petrova, I.A. Prudaev, T.M. Yaskevich, Semiconductors 49 (2015) 345.
[14] V.M. Kalygina, V.A. Novikov, Y.S. Petrova, O.P. Tolbanov, E.V. Chernikov, S.Y. Tsupy, T.M. Yaskevich, Semiconductors 48 (2014) 961.
[15] V.M. Kalygina, V.A. Novikov, Y.S. Petrova, O.P. Tolbanov, E.V. Chernikov, S.Y. Tcupiy, T.M. Yaskevich, Semiconductors 48 (2014) 739.
[16] V.M. Kalygina, Y.S. Petrova, I.A. Prudaev, O.P. Tolbanov, S.Y. Tsupiy, Semiconductors 49 (2015) 1012.
[17] M. Lampert, P. Mark, Injection Currents In Solids, Mir, Moscow, 1973.
[18] D. Wei, T. Hossain, N.Y. Garces, N. Nepal, H.M. Meyer, M.J. Kirkham, C.R. Eddy Jr., J.H. Edgar, ESC J. Solid State Sci. Technol. 2 (2013) 110.
[19] S. Sze, Physics of Semiconductor Devices, v. 1, Mir, Moscow, 1984.
[20] V.I. Gaman, Physics Of Semiconductor Devices, Nauka, Novosibirsk, 2000.